Eksakta : Berkala Ilmiah Bidang MIPA
VOLUME 26 NO 04 2025, pp 500-515
ISSN : Print 1411-3724 — Online 2549-7464
DOI : https://doi.org/10.24036/eksakta/vol26-iss04/627

Eksakta
Berkala Ilmiah Bidang MIPA
http://www.eksakta.ppj.unp.ac.id/index.php/eksakta

Article

Synthesis and Characterization of Sodium Aluminate from Aluminum and Sodium Hydroxide

Article Info

Article history :
Received September 26, 2025
Revised Novenber 10, 2025
Accepted November 14, 2025
Published December 30, 2025
In Press

Keywords :
Sodium aluminate,
synthesis,
aluminum,
sodium hydroxide
characterization

Dinalia Dinalia[1*], Syamsi Aini[2], Jon Efendi[2]

[1]Department of Chemistry, Faculty of Mathematics and Natural Science, Tadulako University, Palu, Indonesia
[2]Department of Chemistry, Faculty of Mathematics and Natural Science, State University of Padang, Padang, Indonesia

Abstract. The synthesis of sodium aluminate from aluminum and sodium hydroxide was successfully conducted to optimize its potential as a precursor for zeolite production. Aluminum was reacted with NaOH solution under continuous stirring for five hours, with variations in pH and Al-to-NaOH molar ratio to determine optimal synthesis conditions. The highest aluminum conversion (94.33%) was achieved at pH 13.6 and an Al-to-NaOH molar ratio of 1:4. Fourier-transform infrared (FTIR) spectroscopy confirmed the formation of tetrahedral $[AlO_4]^-$ units through characteristic aluminate vibrational bands at 624 and 727 cm^{-1}. X-ray diffraction (XRD) analysis revealed sharp reflections at $2\theta \approx 34.8°$, corresponding to crystalline $NaAlO_2$ (JCPDS No. 33-1200), indicating high crystallinity and phase purity. Scanning electron microscopy coupled with energy-dispersive X-ray (SEM–EDX) analysis showed irregular plate-like crystalline particles with a near-stoichiometric Na:Al ratio (~1:1), confirming compositional homogeneity. Overall, optimized alkalinity and stoichiometry were found to be critical for producing highly crystalline and compositionally pure sodium aluminate, suggesting its suitability as a high-quality, environmentally friendly precursor for zeolite synthesis.

Corresponding Author :
Dinalia Dinalia
Department of Chemistry, Faculty of Mathematics and Natural Science,
Tadulako University, Palu, Indonesia
Email : dinalia@untad.ac.id

1. Introduction

Sodium aluminate is a commercially important inorganic chemical with significant applications across various industrial sectors. It is utilized in water treatment [1], refractory brick production [2], construction materials [3], the paper industry [4], and as as a precursor for alumina [5]. In addition, sodium aluminate serves as a fundamental intermediate in the synthesis of zeolite [6]. Among various alumina sources, sodium aluminate has been identified as the most effective precursor for nanosized ZSM-5 synthesis, yielding a higher degree of crystallinity than other alumina sources such as alumina, aluminum hydroxide, or aluminum sulfate [7].

Various approaches for sodium aluminate synthesis have been reported in the literature, including synthesis from basic aluminum sulfate (BAS) [8], alum waste [9], bauxite residue [10], aluminum nitrate solution [11], and saline slag waste [12]. Most previous studies, however, have employed aluminum hydroxide ($Al(OH)_3$) as the primary aluminum source for sodium aluminate preparation [13]. Several researchers have noted that the characterization of zeolite 4A synthesized using $Al(OH)_3$ as the aluminat source revealed that aluminum hydroxide (gibbsite) remained the dominant phase rather than zeolite [14], while others found that $Al(OH)_3$ could still yield zeolite 4A in greater quantities than residual aluminum hydroxide [15]. These conflicting findings indicate that the synthesis conditions of sodium aluminate strongly influence the quality and crystallinity of zeolite products derived from it. Hence, optimizing sodium aluminate synthesis is crucial to ensure that the precursor possesses the appropriate structural and compositional characteristics for zeolite formation.

Meanwhile, aluminum is abundantly available in daily life due to its widespread use in various applications, such as household utensils, food and beverage packaging, cosmetics [16] pharmaceuticals [17], and perfume containers [18]. Aluminum waste may contribute to increasing environmental burdens, If not properly recycled or reused. [19]. However, aluminum derived from such waste can serve as an alternative source for sodium aluminate synthesis [20]. Converting aluminum into sodium aluminate not only provides an efficient utilization pathway for readily available aluminum but also supports circular economy principles in material chemistry.

Despite the industrial importance of sodium aluminate, limited studies have focused on synthesizing it directly from aluminum metal under controlled alkaline conditions. The reaction between aluminum and sodium hydroxide offers a straightforward route for sodium aluminate formation, but the process efficiency is highly dependent on solution alkalinity (pH) and the molar ratio of aluminum to NaOH. These two parameters determine the degree of aluminum dissolution, the phase stability of aluminate ions $[Al(OH)_4]^-$, and the crystallinity of the resulting solid [21]. However, systematic investigation of these parameters has rarely been reported, leaving a gap in understanding the optimal conditions for obtaining highly reactive sodium aluminate suitable for zeolite synthesis.

Therefore, this study aims to investigate the synthesis of sodium aluminate from aluminum and sodium hydroxide solution by systematically examining the effects of NaOH solution pH and the Al-to-NaOH molar ratio on the percentage of reacted aluminum. These two parameters were selected as the primary variables because they directly determine the equilibrium between solid $Al(OH)_3$ and soluble aluminate species, thereby controlling the reaction yield and the phase purity of the resulting sodium aluminate. The synthesized product was characterized using FTIR, XRD, and SEM–EDX to confirm its structural and compositional properties. This work provides an important contribution by establishing the relationship between synthesis parameters and the structural characteristics of sodium aluminate, offering new insights for optimizing precursors in zeolite synthesis.

2. Experimental Section

The synthesis of sodium aluminate in this study was performed by modifying the procedures reported in previous works [22], with theoretical considerations adapted from [13]. All experiments were conducted in triplicate to ensure reproducibility, and the average values were reported. The

experimental error for aluminum conversion was maintained within ±2%. Analytical-grade reagents were used throughout the study, including sodium hydroxide (NaOH, ≥99%, Merck) and aluminum metal powder (Al, 99.5% purity, Sigma–Aldrich), and oxalic acid dihydrate (≥99.5%, Merck). Distilled water was used for all preparations. All glassware was rinsed with distilled water and oven-dried before use.

2.1 Effect of NaOH Solution pH on the Synthesis of Sodium Aluminate

A series of NaOH solutions with pH values ranging from 13.0 to 14.0 were prepared to investigate the influence of alkalinity on sodium aluminate formation. Each solution (100 mL) was prepared by dissolving analytical-grade NaOH in distilled water. Theoretical pH values were estimated based on hydroxide ion concentration under the assumption of complete dissociation and were verified experimentally by titration against standardized oxalic acid using phenolphthalein as an indicator. To ensure accuracy at highly alkaline media, pH estimation followed the non-ideal ionic activity correction described in [23].

Aluminum powder was reacted with each NaOH solution at a concentration equivalent to 0.1 M aluminum. The reaction was conducted in a branched Erlenmeyer flask connected to a water vacuum system to continuously remove the generated hydrogen gas and prevent CO_2 ingress. Each reaction proceeded for 5 h under continuous magnetic stirring at approximately 600 rpm and ambient laboratory temperature. After completion, the mixture was immediately filtered using Whatman No. 42 filter paper to separate the solid residue from the filtrate. The residue was washed thoroughly with distilled water, dried, and weighed to determine the mass of unreacted aluminum. The filtrate was evaporated at 120 °C to obtain the sodium aluminate solid. The percentage of aluminum that reacted (% Al reacted) was calculated was calculated from the difference between the initial and residual aluminum masses using equation 1:

$$\%\ Al\ reacted = \frac{m_i - m_r}{m_i} x100\% \qquad (1)$$

where m_i is the initial mass of aluminum (g) and m_r is the mass of unreacted residue (g).

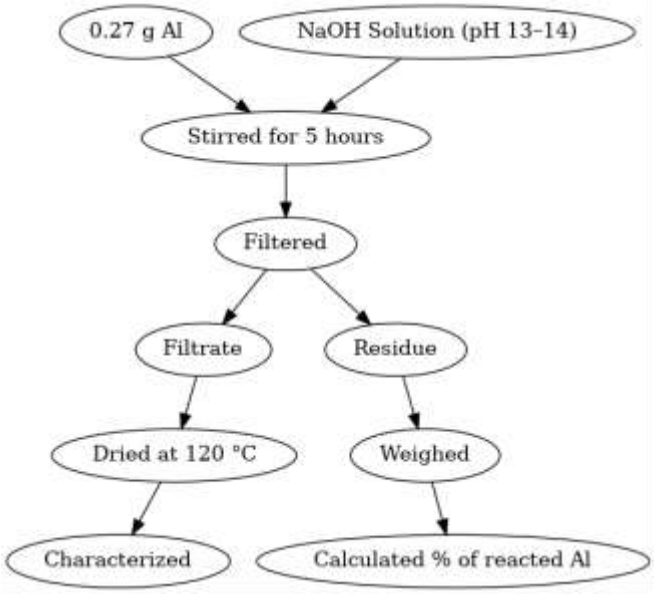

Figure 1. Schematic workflow of the effect of NaOH solution pH on aluminum reaction yield

2.2 Effect of Aluminum-to-NaOH Molar Ratio on the Synthesis of Sodium Aluminate

To examine the effect of stoichiometric composition on the formation of sodium aluminate, aluminum was reacted with NaOH solutions at different molar ratios of Al to NaOH, ranging from 1:1 to 1:5. The NaOH solution used corresponded to the pH condition that yielded the highest percentage of reacted aluminum in the preliminary experiment. Each reaction was performed in a 100 mL solution under the same conditions as described in Section 2.1.

The reactions were conducted in a branched Erlenmeyer flask connected to a water vacuum system to continuously remove hydrogen gas and prevent carbon dioxide ingress during the process. Each experiment was carried out for 5 h under constant magnetic stirring at approximately 600 rpm and ambient temperature. Upon completion, the mixtures were immediately filtered using Whatman No. 42 filter paper to separate the solid residue from the filtrate. The solid residue was washed with distilled water, dried, and weighed to determine the unreacted aluminum. The filtrate was evaporated at 120 °C to yield the sodium aluminate solid.

The percentage of aluminum reacted (% Al reacted) at each molar ratio was calculated using Equation (1), as described previously in Section 2.1. The obtained data were used to determine the molar ratio condition that resulted in the highest aluminum conversion, providing the optimum stoichiometric balance between aluminum and sodium hydroxide for sodium aluminate synthesis.

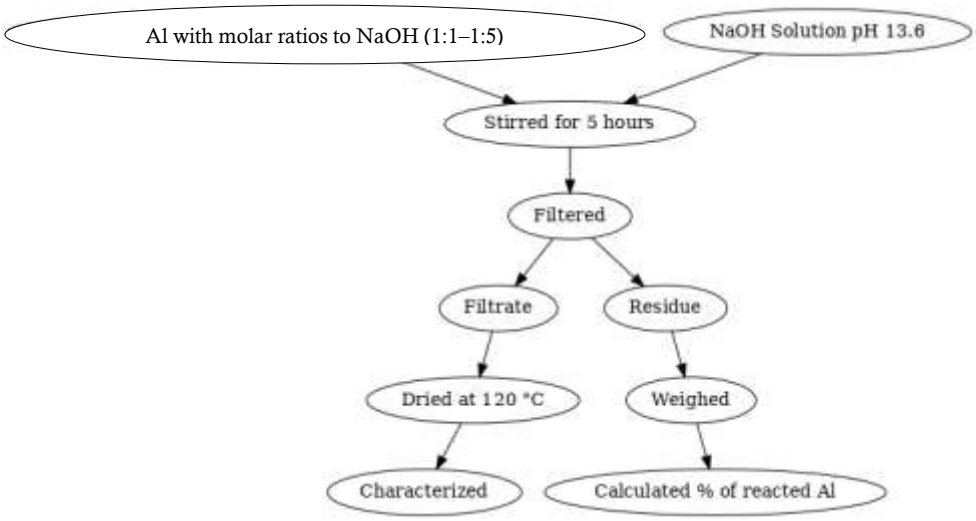

Figure 2. Schematic workflow of the effect of Al-to-NaOH molar ratio on aluminum reaction yield

2.3 Characterization of Sodium Aluminate and Analysis

The solid sodium aluminate products obtained under the optimum synthesis conditions were characterized using several analytical techniques to confirm their structure, crystallinity, morphology, and elemental composition.

2.3.1 Fourier Transform Infrared (FTIR) Spectroscopy

The infrared spectra of the synthesized sodium aluminate samples were recorded using a Shimadzu IRPrestige-21 Fourier Transform Infrared Spectrophotometer within the wavenumber range of 4000–400 cm^{-1}, employing the KBr pellet method. Each sample was finely ground, mixed with spectroscopic-grade KBr (1:100 mass ratio), and pressed into a thin pellet prior to analysis. The spectra were collected at a resolution of 4 cm^{-1} with 32 scans per sample. The observed absorption bands were analyzed to identify the characteristic vibrational modes of the aluminate ion, particularly ν_1 (symmetric stretching), ν_2 (symmetric bending), ν_3 (asymmetric stretching), and ν_4 (asymmetric

bending). The presence of these characteristic absorption bands confirms the formation of sodium aluminate with typical tetrahedral AlO_4 structural units [24].

2.3.2 X-ray Diffraction (XRD) Analysis

Phase identification and crystallinity determination of the sodium aluminate solids were performed using an X-ray diffractometer (PANalytical X'Pert PRO) equipped with Cu Kα radiation (λ = 1.5406 Å), operated at 40 kV and 30 mA. Diffraction data were collected over a 2θ range of 10°–80° at a scanning rate of $2°\cdot min^{-1}$. The obtained diffraction patterns were compared with reference data from the Joint Committee on Powder Diffraction Standards (JCPDS) database to identify crystalline phases corresponding to $NaAlO_2$ and possible residual aluminum hydroxide phases.

2.3.3 Scanning Electron Microscopy–Energy Dispersive X-ray (SEM–EDX) Analysis

Morphological and elemental analyses were carried out using a JEOL JSM-6510LA Scanning Electron Microscope equipped with an Oxford EDX detector. The samples were mounted on aluminum stubs and coated with a thin layer of gold to improve surface conductivity. SEM micrographs were obtained at various magnifications (500× to 5000×) under an accelerating voltage of 20–30 kV. The EDX spectra were recorded simultaneously to determine the elemental composition and verify the presence of sodium (Na) and aluminum (Al) as major constituents, along with minor oxygen (O) peaks corresponding to the formation of sodium aluminate. The EDX data were used semi-quantitatively to estimate the atomic percentage of each element and to confirm compositional homogeneity across the sample surface [25] [26].

3. Results and Discussion

The synthesis of sodium aluminate from aluminum and sodium hydroxide solution was evaluated through two key process variables: the NaOH solution pH and the Al-to-NaOH molar ratio. The percentage of reacted aluminum was used as the main quantitative indicator of conversion efficiency. The optimized product was characterized by FTIR to confirm its structural identity, XRD Analysis to determination of phase identification and crystallinity, and SEM-EDX to analysis of morphological and elemental.

3.1 Effect of NaOH Solution pH on Aluminum Reaction Yield (%)

The dissolution of aluminum in sodium hydroxide proceeds through a redox reaction in which aluminum metal is oxidized to aluminate, while water is reduced to hydrogen gas, as expressed in reaction:

$$2Al_{(s)} + 2NaOH_{(aq)} + 6H_2O_{(l)} \rightarrow 2Na[Al(OH)_4]_{(aq)} + 3H_{2(g)}$$

The reaction efficiency is highly dependent on the hydroxide ion concentration, which controls both the dissolution rate of aluminum and the stability of the aluminate ion $[Al(OH)_4]^-$. Theoretical and experimental studies indicate that tetrahedral aluminate species dominate in strongly alkaline media (pH > 13), whereas at lower pH values, hydrolysis and precipitation of aluminum hydroxide ($Al(OH)_3$) become significant [13]. To examine this effect, NaOH solutions with pH values between 13.0 and 14.0 were prepared, and the percentage of aluminum reacted was determined for each condition.

The synthesis process was carried out by reacting aluminum with sodium hydroxide solution in a branched erlenmeyer flask connected to a water vacuum system to release H_2 gas and prevent CO_2 from entering the solution during the 5-hour reaction. This precaution was necessary because sodium aluminate readily reacts with atmospheric CO_2 to form a white $Al(OH)_3$ precipitate [27] as represented by the following reaction:

$$Al(OH)_{4\,(aq)} + CO_{2\,(g)} \rightarrow Al(OH)_{3\,(s)} + HCO_{3\,(aq)}^-$$

The formation of aluminate was evidenced by the release of gas and the initial appearance of a white precipitate, which subsequently transformed into a clear solution as the reaction progressed. This behavior indicates the conversion of $Al(OH)_3$ precipitate into soluble sodium aluminate [28]. The results of sodium aluminate synthesis under varying NaOH solution pH values and their effect on the percentage of reacted aluminum are presented in Table 1 below:

Table 1. Effect of NaOH solution pH on aluminum reaction yield (%)

H	Aluminum Reaction Yield (%)	Experimental pH
13	81.21	13.15
13.2	84.78	13.27
13.4	86.33	13.49
13.6	88.52	13.66
13.8	87.99	13.87

From the data in Table 1, the effect of NaOH solution pH on aluminum reaction yield (%) is depicted in Figure 3.

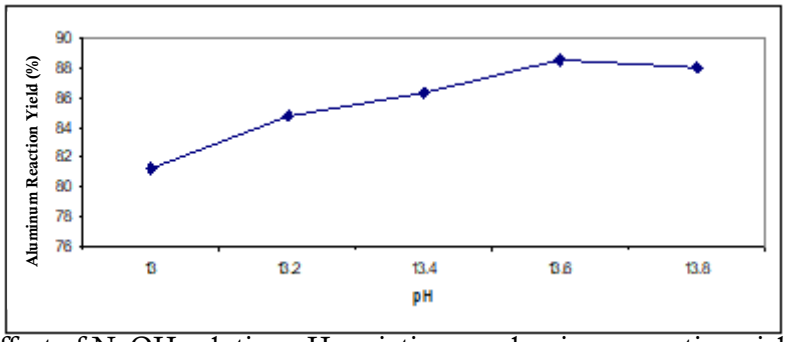

Figure 3. Effect of NaOH solution pH variation on aluminum reaction yield (%)

Analysis of the data presented in Figure 3 indicates that the proportion of aluminum reacted increases with rising NaOH solution pH. The reaction achieved its maximum efficiency at pH 13.6, where the percentage of aluminum conversion was higher than at pH 13.8, establishing pH 13.6 as the optimum condition for aluminum dissolution. This result aligns with the structure of the aluminate ion, $[Al(OH)_4]^-$, where the Al-to-NaOH molar ratio under these conditions corresponds to 1:4. Accordingly, the results confirm that sodium aluminate is formed under excess NaOH conditions [24] as represented by the following reaction:

$$Al_{(s)} \xrightarrow{3OH^-} Al(OH)_{3(s)} \xrightarrow{OH^-} [Al(OH)_4]^-_{(aq)}$$

As the percentage of reacted aluminum remained at 88.52%, the investigation was subsequently continued by examining the effect of varying the Al-to-NaOH molar ratio.

3.2 Effect of Al-to-NaOH Molar Ratio on Aluminum Reaction Yield (%)

The effect of the Al-to-NaOH molar ratio on the conversion efficiency of aluminum to sodium aluminate was systematically investigated to determine the optimal stoichiometric conditions for the reaction. The dissolution of aluminum in sodium hydroxide follows the same mechanism described previously, where aluminum reacts with hydroxide ions to form soluble aluminate species $[Al(OH)_4]^-$ and hydrogen gas.

This stoichiometric equation demonstrates that two moles of aluminum require two moles of NaOH and six moles of water to form sodium aluminate in solution. The $[Al(OH)_4]^-$ ion represents

the predominant aluminate species under strongly alkaline conditions (pH > 13). The extent of this redox process is highly dependent on the molar ratio between aluminum and NaOH, which determines both the hydroxide ion availability and the system's overall alkalinity. Insufficient hydroxide concentration results in incomplete aluminum dissolution and precipitation of $Al(OH)_3$, while excessive NaOH can alter solution viscosity and ionic strength, reducing mass transfer efficiency.

To evaluate this relationship, the synthesis was carried out at the previously determined optimum NaOH solution pH of 13.6. The molar ratio of aluminum to NaOH was systematically varied from 1:1 to 1:5, and the corresponding percentage of reacted aluminum was calculated using Equation (1). The experimental results are summarized in Table 2 and graphically illustrated in Figure 4.

Table 2. Effect of Al-to-NaOH molar ratio on aluminum reaction yield (%)

Al-to-NaOH Molar Ratio	Aluminum Reaction Yield (%)	Experimental pH
1:1	19.53	13.71
1:2	92.48	13.64
1:3	92.76	13.72
1:4	94.33	13.66
1:5	93.94	13.70

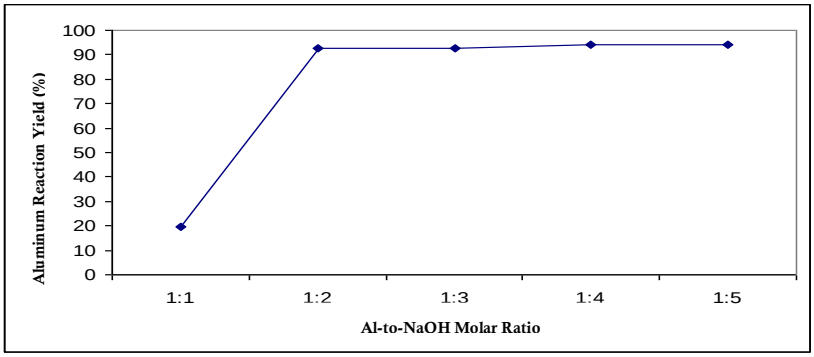

Figure 4. Effect of Al-to-NaOH molar ratio variation on aluminum reaction yield (%)

A significant increase in aluminum conversion is observed as the molar ratio rises from 1:1 to 1:2. This behavior reflects the critical role of hydroxide concentration in facilitating the oxidative dissolution of aluminum and stabilizing the aluminate ion in solution. At the 1:1 ratio, the dissolution of aluminum is limited because hydroxide ions are rapidly consumed near the metal surface, forming a transient $Al(OH)_3$ film that inhibits further reaction. This demonstrates that NaOH was insufficient to sustain the conversion of $Al(OH)_3$ into soluble $[Al(OH)_4]^-$ ions [21].

In contrast, at higher ratios (1:2–1:5), aluminum dissolution continued to increase as the equilibrium shifted toward aluminate ion formation. The dissolution behavior can be explained by the following reaction:

$$Al(OH)_{3\,(s)} + OH^-_{(aq)} \leftrightarrow [Al(OH)_4]^-_{(aq)}$$

This reaction is reversible, and the direction of the reaction depends strongly on hydroxide concentration. At lower OH^- concentrations, the reaction shifts to the left, leading to precipitation of $Al(OH)_3$. Conversely, at sufficiently high NaOH concentrations (around a 1:4 ratio), the equilibrium is driven to the right, favoring complete formation of soluble aluminate ions $[Al(OH)_4]^-$. However,

when the ratio was further increased to 1:5, no significant improvement in aluminum yield was observed. This behavior suggests that beyond the stoichiometric requirement, excess OH^- no longer contributes to aluminum dissolution and may even induce local supersaturation, slightly reducing the effective reaction rate due to the formation of a dense passivation layer at the metal surface [25].

This observation is consistent with the stoichiometric reaction pathway and with prior studies that identified an optimal hydroxide excess (Al:NaOH ≈ 1:4) for maximizing aluminum conversion and preventing precipitation of intermediate hydroxides [13]. The overall findings confirm that the Al-to-NaOH molar ratio of 1:4 represents the most chemically efficient condition for sodium aluminate synthesis under the studied parameters, yielding the highest percentage of reacted aluminum (94.33%). This ratio provides a balance between sufficient hydroxide ion availability and controlled reaction kinetics, supporting the formation of stable tetrahedral $[Al(OH)_4]^-$ species in solution prior to solid sodium aluminate formation upon drying.

When the reaction mixture is subsequently dried or heated, the hydrated aluminate dehydrates to produce solid sodium aluminate ($NaAlO_2$), as represented by:

$$Na[Al(OH)_4]_{(aq)} \rightarrow NaAlO_{2\,(s)} + 2H_2O_{(l)}$$

It should be noted that minor variations in aluminum yield may arise from filtration losses or weighing uncertainties of the unreacted residue. However, replicate measurements exhibited a standard deviation below ±2%, confirming good reproducibility and reliability of the experimental data. To gain further insight into the structure of the sodium aluminate formed under this condition, the resulting solid was characterized by infrared spectroscopy.

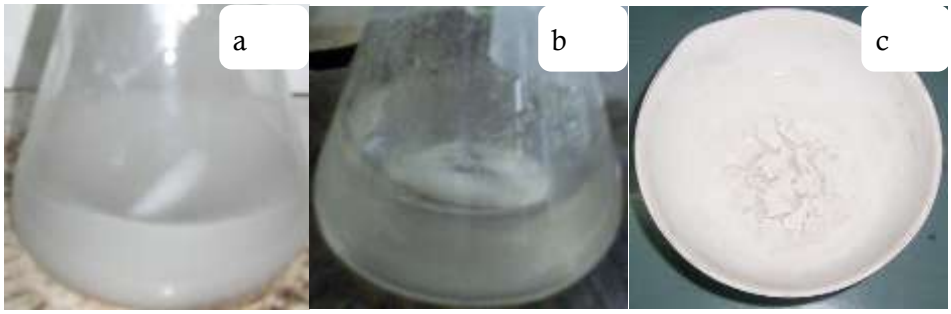

Figure 5. Sequential stages in sodium aluminate synthesis: (a) Formation of $Al(OH)_3$ precipitate from the aluminum-NaOH reaction; (b) Dissolution of the precipitate into clear sodium aluminate solution; (c) Solid sodium aluminate obtained after drying at 120 °C.

3.3 Characterization by Infrared Spectroscopy

Infrared spectroscopy was employed to confirm the structural formation of sodium aluminate synthesized under the optimum reaction conditions (NaOH solution pH 13.6 and an Al-to-NaOH molar ratio of 1:4). The FTIR spectrum of the obtained solid sample is presented in Figure 6. Characteristic absorption bands corresponding to the aluminate ion were observed, confirming the successful formation of sodium aluminate.

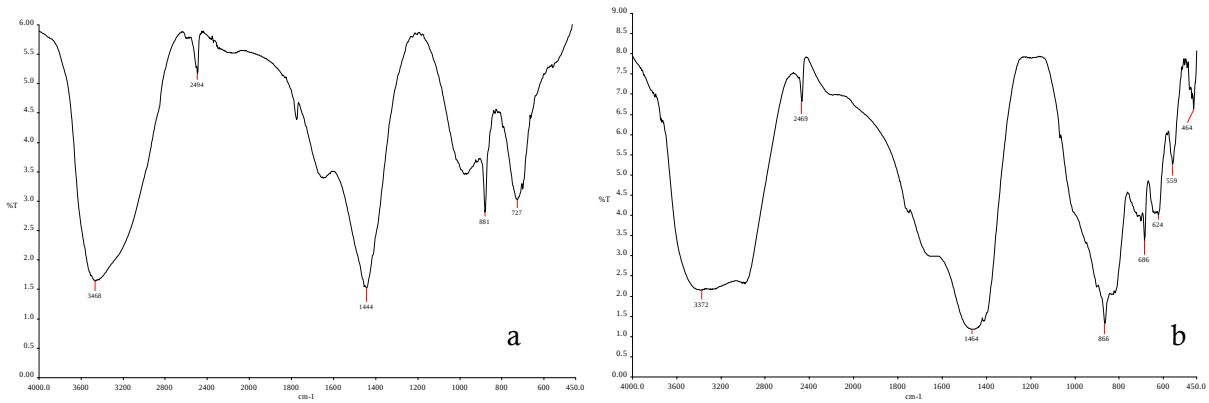

Figure 6. FTIR spectra of sodium aluminate synthesized at pH 13.6 (a) and Al-to-NaOH molar ratio 1:4 (b).

The main vibrational bands appeared at 727 cm^{-1} and 624 cm^{-1}, which correspond to the asymmetric (ν_3) and symmetric (ν_1) stretching vibrations of the Al–O bond within the tetrahedral AlO_4 unit. These two bands are typical of sodium aluminate and consistent with previous studies that reported strong absorptions around 720–700 cm^{-1} for asymmetric Al–O stretching and 620–630 cm^{-1} for symmetric stretching modes in alkaline aluminate systems. The tetrahedral $[AlO_4]^-$ ion exhibits four fundamental vibrational modes, namely ν_1 (symmetric stretching), ν_2 (symmetric bending), ν_3 (asymmetric stretching), and ν_4 (asymmetric bending), located at 615, 310, 720, and 310 cm^{-1}, respectively [24].

The FTIR data obtained in this study are summarized in Table 3, including the observed wavenumbers and their corresponding vibrational assignments. The ν_2 and ν_4 bending modes could not be detected due to instrumental limitations, as the spectrometer's operational range (4000–400 cm^{-1}) does not extend to the lower-frequency region near 310 cm^{-1}. Previous spectroscopic investigations have reported that the ~310 cm^{-1} band of aluminate ions is often weak and undetectable under standard IR conditions [24].

The broad band observed between 3640 and 3430 cm^{-1} represents O–H stretching vibrations arising from residual hydroxyl groups and adsorbed moisture [29], while the band at ~1630 cm^{-1} corresponds to H–O–H bending of interstitial water molecules. These features confirm that the synthesized sodium aluminate retains a degree of hydration, as expected for materials dried below 150 °C. The weak band near 450 cm^{-1} is associated with Al–O–Al bending vibrations, indicating partial polymerization within the alumina framework [30].

Table 3. Characteristic infrared absorption bands of sodium aluminate. Source: Own data, 2025.

Wavenumber (cm^{-1})	Vibration Mode	Assignment
3640-3430	ν(O–H) stretching	Hydroxyl groups in adsorbed water / Al–OH groups
1650-1630	δ(H–O–H) bending	Molecular water (H_2O)
727	ν_3 asymmetric stretching	Al–O bond in tetrahedral $[AlO_4]$ units
624	ν_1 symmetric stretching	Al–O bond in tetrahedral $[AlO_4]$ units
470-450	lattice vibration	Al–O–Al linkage deformation

In addition, the presence of these characteristic absorption bands confirms the formation of sodium aluminate with tetrahedral $[AlO_4]^-$ structural units. The absence of broad O–H stretching around 3400 cm^{-1} and Al–OH bending near 950 cm^{-1} further indicates that no residual aluminum hydroxide ($Al(OH)_3$) was present in the final product [31]. Thus, the FTIR results demonstrate that the reaction between aluminum and NaOH at solution pH 13.6 and an Al-to-NaOH molar ratio of 1:4 successfully produced sodium aluminate with a well-defined tetrahedral framework.

Although FTIR analysis provided clear evidence of aluminates' vibrational features, it cannot determine the crystallinity or distinguish polymorphic phases of $NaAlO_2$. Therefore, complementary structural analysis using X-ray diffraction (XRD) was conducted to confirm phase identity and crystallinity of the synthesized material.

3.4 XRD Characterization and Phase Identification

X-ray diffraction (XRD) analysis was conducted to identify the crystalline phases and evaluate the degree of crystallinity of the synthesized sodium aluminate solids. The obtained diffraction patterns were compared with standard reference data from the Joint Committee on Powder Diffraction Standards (JCPDS) database, specifically card No. 33-1200 corresponding to $NaAlO_2$ [32].

The XRD pattern of sodium aluminate synthesized at pH 13.6 (Figure 7) exhibits multiple diffraction peaks at 2θ = 15.77°, 20.89°, 21.47°, 34.71°, 40.03°, 44.13°, and 54.29°, indicating the presence of partially crystalline sodium aluminate. The main peaks at 34.71° and 40.03° correspond to the (211) and (220) crystal planes of $NaAlO_2$ (JCPDS No. 33-1200) [32], confirming that the product predominantly consists of crystalline sodium aluminate. However, the additional weaker peaks suggest the coexistence of minor secondary or amorphous phases, possibly hydrated alumina ($Al(OH)_3$) or sodium hydroxide hydrates, which may form under conditions of incomplete aluminum dissolution. The moderate sharpness of the peaks also suggests intermediate crystallinity, as summarized in Table 4.

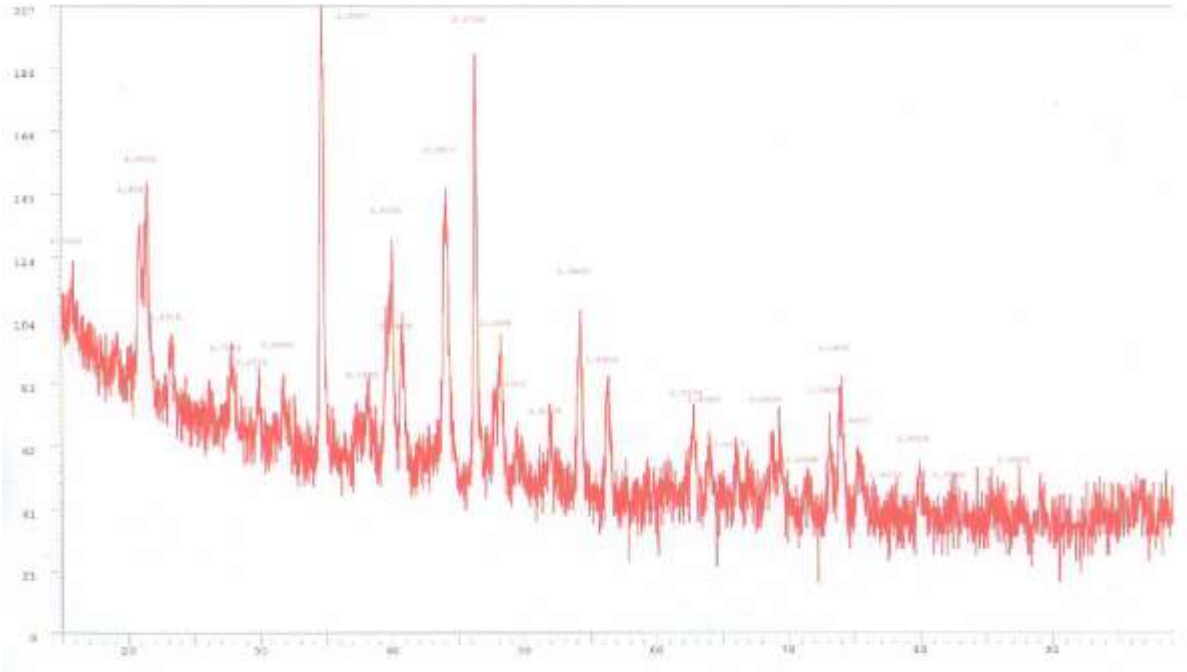

Figure 7. XRD diffractogram of sodium aluminate synthesized at pH 13.6.

Table 4. Main diffraction peaks of sodium aluminate synthesized at pH 13.6

2θ (°)	d-spacing (Å)	Relative Intensity (%)	Assigned Phase
15.77	6.5203	56.5	$NaAlO_2$ (minor)
20.89	4.9340	64.7	$NaAlO_2$
21.47	4.8022	69.6	$Al(OH)_3$ (possible)
34.71	2.9987	97.6	$NaAlO_2$ (211)
40.03	2.6134	61.4	$NaAlO_2$ (220)
44.13	2.3811	71.0	$NaAlO_2$ (311)
54.29	1.9605	51.7	$NaAlO_2$

In contrast, the sample prepared at an Al-to-NaOH molar ratio of 1:4 displayed a much simpler and sharper diffraction pattern (Figure 8), dominated by two intense peaks at 2θ = 34.85° and 34.91°, corresponding to d-spacings of 2.9870 and 2.9820 Å, respectively. These peaks represent the (211) and (220) reflections of $NaAlO_2$, consistent with JCPDS card No. 33-1200 [32]. The narrow and highly intense peaks (87.6% and 98.3%) indicate a well-ordered crystalline structure and suggest that aluminum was almost completely converted into pure sodium aluminate. No additional peaks from aluminum hydroxide or other secondary phases were detected, confirming high phase purity. The detailed diffraction data are presented in Table 5.

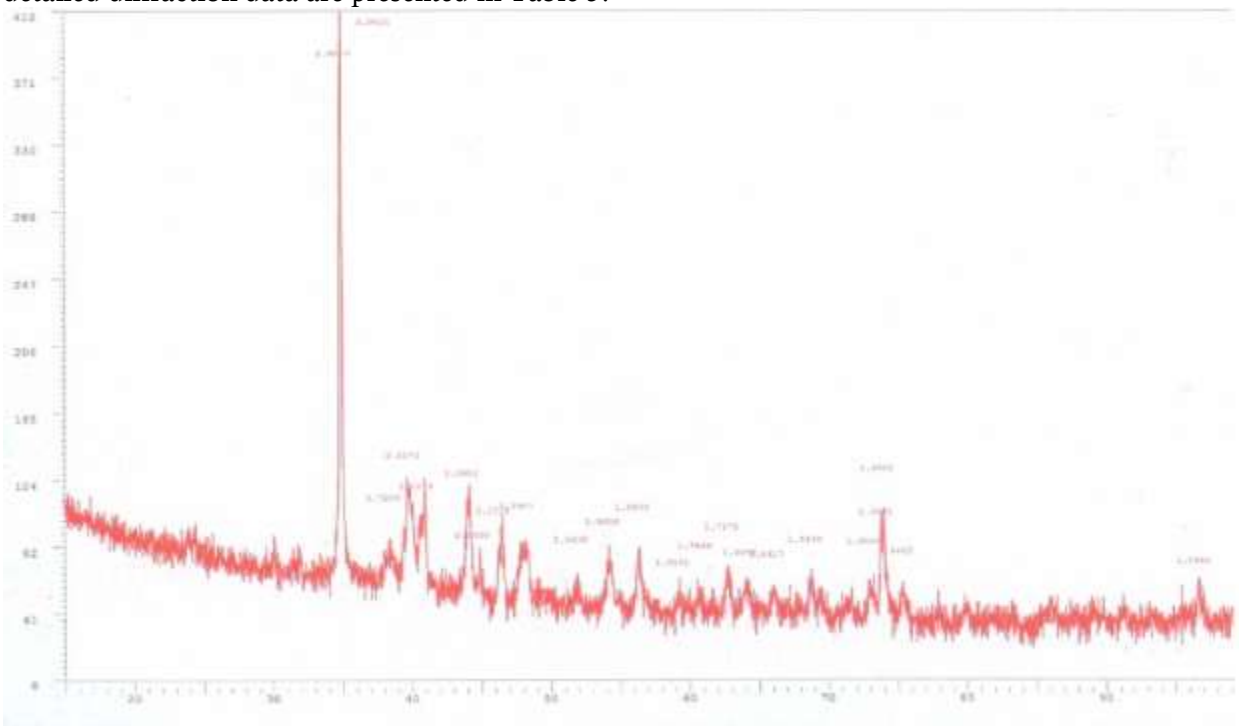

Figure 8. XRD diffractograms of sodium aluminate synthesized at an Al-to-NaOH molar ratio of 1:4.

Table 5. Main diffraction peaks of sodium aluminate synthesized at Al-to-NaOH molar ratio 1:4.

2θ (°)	d-spacing (Å)	Relative Intensity (%)	Assigned Phase
34.85	2.9870	87.6	$NaAlO_2$ (211)
34.91	2.9820	98.3	$NaAlO_2$ (220)

Comparison of both diffraction patterns clearly reveals that the Al-to-NaOH molar ratio of 1:4 produced a material with higher crystallinity and structural uniformity compared to the sample synthesized at pH 13.6. The pH 13.6 sample displayed multiple broad peaks and minor reflections, suggesting the coexistence of amorphous or hydrated alumina species, which typically form when aluminum dissolution is incomplete. Meanwhile, the 1:4 sample exhibited only two sharp, intense peaks at nearly identical 2θ positions (~34.9°), characteristic of well-crystallized $NaAlO_2$ [33]. These results confirm that the molar ratio of 1:4 provides sufficient hydroxide ions for complete formation and stabilization of the $[Al(OH)_4]^-$ species, leading to the precipitation of pure, crystalline sodium aluminate upon drying.

Therefore, the XRD analysis supports the conclusion that the Al-to-NaOH molar ratio of 1:4 yields the most crystalline and phase-pure sodium aluminate, consistent with the highest aluminum conversion (≈94.3%), This result correlates well with the FTIR findings, which confirmed the presence of tetrahedral AlO_4 vibrational modes, providing structural evidence that the obtained $NaAlO_2$ is predominantly crystalline and compositionally pure.

While the XRD results confirmed the phase purity and crystalline structure of the synthesized sodium aluminate, this technique does not provide information about particle morphology or elemental distribution. Therefore, complementary surface and compositional analyses were conducted using Scanning Electron Microscopy coupled with Energy Dispersive X-ray (SEM–EDX) spectroscopy to further characterize the material.

3.5 Morphological and Elemental Characterization by SEM–EDX

Scanning Electron Microscopy (SEM) coupled with Energy Dispersive X-ray (EDX) spectroscopy was performed to investigate the surface morphology and elemental composition of the sodium aluminate sample synthesized under the optimum reaction condition (Al-to-NaOH molar ratio 1:4). The SEM micrograph (Figure 9) reveals that the sodium aluminate product exhibits irregularly aggregated crystalline particles with a plate-like and partially porous morphology, typical of dehydrated $NaAlO_2$ solids. The particles appear to have sizes ranging from approximately 1 to 5 μm, forming agglomerates with rough surface texture. The heterogeneous morphology indicates the partial fusion of smaller crystallites during drying at 120 °C, consistent with the moderate thermal treatment applied after synthesis. Such morphology is characteristic of crystalline sodium aluminate and aligns with previous observations for materials derived from direct aluminum–alkali reactions [22].

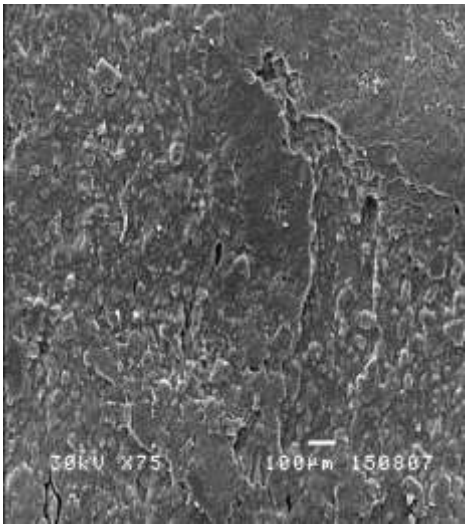

Figure 9. SEM micrograph of sodium aluminate synthesized under optimum conditions (Al-to-NaOH molar ratio 1:4).

The corresponding EDX spectrum (Figure 10) confirms the elemental composition of the sodium aluminate product.

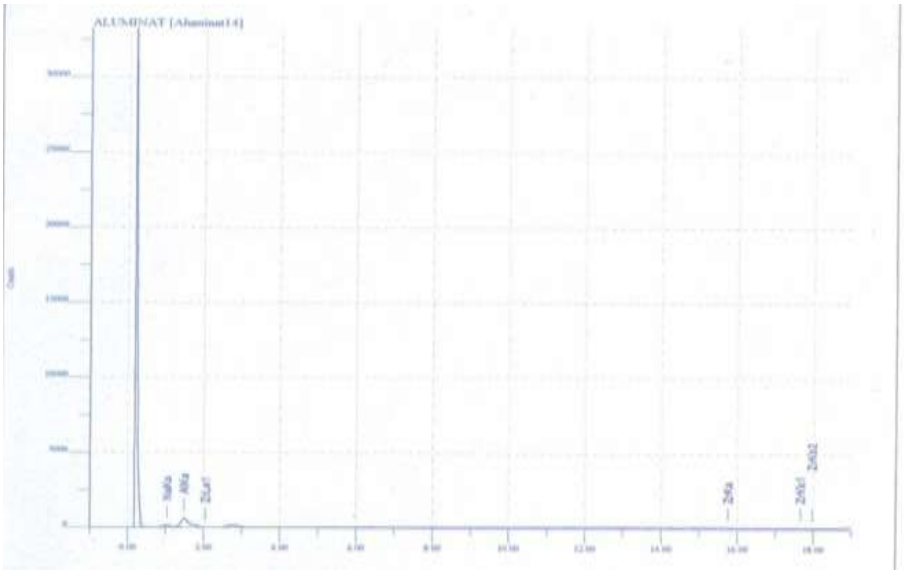

Figure 10. EDX spectrum of sodium aluminate showing characteristic Na Kα, Al Kα, and minor Zr Lα peaks.

The spectrum displays distinct peaks corresponding to sodium (Na Kα, ≈1.05 keV) and aluminum (Al Kα, ≈1.48 keV), indicating the presence of both cations as the main constituents of sodium aluminate. Minor zirconium (Zr Lα, ≈2.04 keV) signals were also detected, likely originating from the sample stub or coating material. The quantitative elemental results are summarized in Table 6.

Table 6. Elemental composition of sodium aluminate determined by EDX.

Element	wt (%)	at/mole (%)	Assigned Compound
Na	49.9400	53.9946	$NaAlO_2$
Al	49.8885	45.9586	$NaAlO_2$
Zr	0.1715	0.0467	Trace (substrate)

The nearly equal weight percentages of sodium and aluminum (Na:Al ≈ 1:1) confirm stoichiometric incorporation consistent with the $NaAlO_2$ composition [34]. Although the atomic percentages (Na:Al ≈ 1.2:1) show a slight deviation, this difference can be attributed to instrumental corrections and the low X-ray yield of sodium. The near-equimolar Na/Al ratio, together with the absence of impurity peaks such as Si, Fe, or Ca, demonstrates high phase purity, consistent with the XRD findings showing only $NaAlO_2$ reflections. The minor trace of zirconium (<0.2 wt%) originates from the substrate and does not influence the chemical composition of the synthesized material.

The SEM–EDX findings corroborate the FTIR and XRD results discussed earlier, which demonstrated that the product synthesized under the 1:4 stoichiometric condition possesses a well-defined tetrahedral $[AlO_4]^-$ structure and high phase purity. The homogeneous distribution of Na and Al across the sample surface further supports the formation of a chemically uniform $NaAlO_2$ phase.

Overall, the SEM–EDX analysis verifies that the sodium aluminate synthesized at an Al-to-NaOH molar ratio of 1:4 possesses a well-crystallized, plate-like morphology and a stoichiometric $NaAlO_2$ composition. Together with the structural (FTIR) and phase (XRD) analyses, these results

demonstrate that the optimized synthesis condition yields a pure, homogeneous, and compositionally balanced sodium aluminate product suitable as a reactive precursor for zeolite formation.

4. Conclusion

The synthesis of sodium aluminate from aluminum and sodium hydroxide solution demonstrated that both the alkalinity (pH) of the NaOH solution and the Al-to-NaOH molar ratio strongly influence the efficiency of aluminum conversion and the phase purity of the resulting product. The optimum synthesis conditions were achieved at pH 13.6 and an Al-to-NaOH molar ratio of 1:4, yielding the highest aluminum reaction efficiency (94.3%).

Characterization by FTIR confirmed the formation of tetrahedral $[AlO_4]^-$ structural units through the appearance of characteristic aluminate vibrational bands at 624 and 727 cm^{-1}. Complementary XRD analysis revealed sharp diffraction peaks at $2\theta \approx 34.8°$, corresponding to $NaAlO_2$ crystalline planes (JCPDS No. 33-1200), indicating high crystallinity and the absence of secondary hydroxide phases. Furthermore, SEM–EDX analysis verified that the product possessed a plate-like crystalline morphology with a near-stoichiometric Na:Al ratio (~1:1), confirming a homogeneous and compositionally pure $NaAlO_2$ phase.

The integration of these findings demonstrates that optimized alkalinity and stoichiometry are critical to achieving complete aluminum conversion and producing highly crystalline sodium aluminate with uniform structural and elemental characteristics. Such a material is a promising precursor for the synthesis of environmentally friendly zeolites, where structural uniformity and high phase purity are essential for controlling framework composition and catalytic performance.Future research should further investigate the influence of synthesis temperature and reaction kinetics on the crystalline structure and particle morphology of sodium aluminate, as well as evaluate its reactivity and performance in zeolite formation under sustainable synthesis conditions.

References

[1] de Jesus, J. O. N., Medeiros, D. L., Esquerre, K. P. O., Sahin, O., & de Araujo, W. C. (2024). Water treatment with aluminum sulfate and tanin-based biocoagulant in an oil refinery: the technical, environmental, and economic performance. *Sustainability*, *16*(3), 1191.

[2] Adesanya, E., Perumal, P., Luukkonen, T., Yliniemi, J., Ohenoja, K., Kinnunen, P., & Illikainen, M. (2021). Opportunities to improve sustainability of alkali-activated materials: A review of side-stream based activators. *Journal of Cleaner Production*, *286*, 125558.

[3] Ri, J. H., Pak, Y. S., & Yun, K. S. (2020). Preparation Of Cement Grinding Aids Based On Alumina Compounds. *Bilimsel Madencilik Dergisi*, *59*(2), 123-129.

[4] Ming, X., Li, Q., & Jiang, W. (2021). Application of Aluminum Sulfate in the Treatment of Papermaking White Water. *BioResources*, *16*(1).

[5] Damjanovic, V., Filipovic, R., Obrenovic, Z., Perusic, M., Kostic, D., Smiljanic, S., & Stopic, S. (2023). Influence of process parameters in three-stage purification of aluminate solution and aluminum hydroxide. *Metals*, *13*(11), 1816.

[6] Rozhkovskaya, A., Rajapakse, J., & Millar, G. J. (2021). Optimisation of zeolite LTA synthesis from alum sludge and the influence of the sludge source. *Journal of Environmental Sciences*, *99*, 130-142.

[7] Awala, H., Kunjir, S. M., Vicente, A., Gilson, J. P., Valtchev, V., Seblani, H., ... & Mintova, S. (2021). Crystallization pathway from a highly viscous colloidal suspension to ultra-small FAU zeolite nanocrystals. *Journal of Materials Chemistry A*, *9*(32), 17492-17501.

[8] Zhao, Y., Zheng, Y., Peng, Y., He, H., & Sun, Z. (2021). Characteristics of poly-silicate aluminum sulfate prepared by sol method and its application in Congo red dye wastewater treatment. *RSC advances*, *11*(60), 38208-38218.

[9] U. Medhat, T. A. M. Abd El Razek, and A. M. Abd Elbasier. (2024). Production of Sodium Silicate and Sodium Aluminate From Alum Production Waste, *J. Environ. Sci.*, vol. 53, no. 3.
[10] Cheng, L., Wang, Y., Wang, B., Qi, T., Liu, G., Zhou, Q., ... & Li, X. (2022). Phase transformation of desilication products in red mud dealkalization process. *Journal of Sustainable Metallurgy*, *8*(1), 541-550.
[11] Liu, S., Liu, Z., Yan, H., Li, M., & Xia, C. (2023). Desulfurization by Adding Sodium Nitrate in the Production of Alumina from High-Sulfur Bauxite. *JOM: The Journal of The Minerals, Metals & Materials Society (TMS)*, *75*(5).
[12] Yoldi, M., Fuentes-Ordoñez, E. G., Korili, S. A., & Gil, A. (2019). Efficient recovery of aluminum from saline slag wastes. *Minerals Engineering*, *140*, 105884.
[13] Graham, T. R., Hu, J. Z., Jaegers, N. R., Zhang, X., Pearce, C. I., & Rosso, K. M. (2022). An amorphous sodium aluminate hydrate phase mediates aluminum coordination changes in highly alkaline sodium hydroxide solutions. *Inorganic Chemistry Frontiers*, *9*(24), 6344-6357.
[14] Ibsaine, F., Azizi, D., Dionne, J., Tran, L. H., Coudert, L., Pasquier, L. C., & Blais, J. F. (2023). Conversion of aluminosilicate residue generated from lithium extraction process to NaX zeolite. *Minerals*, *13*(12), 1467.
[15] Yoldi, M., Fuentes-Ordoñez, E. G., Korili, S. A., & Gil, A. (2020). Zeolite synthesis from aluminum saline slag waste. *Powder Technology*, *366*, 175-184.
[16] Tietz, T., Lenzner, A., Kolbaum, A. E., Zellmer, S., Riebeling, C., Gürtler, R., ... & Hensel, A. (2019). Aggregated aluminium exposure: risk assessment for the general population. *Archives of toxicology*, *93*(12), 3503-3521.
[17] Lamparelli, E. P., Marino, M., Szychlinska, M. A., Della Rocca, N., Ciardulli, M. C., Scala, P., ... & Santoro, A. (2023). The other side of plastics: Bioplastic-based nanoparticles for drug delivery systems in the brain. *Pharmaceutics*, *15*(11), 2549.
[18] Sanders, R. E., & Marshall, G. J. (2023). *Aluminum: Technology, Industry, and Applications*. ASM International.
[19] Harmaji, A., Jafari, R., & Simard, G. (2024). Valorization of residue from aluminum industries: a review. *Materials*, *17*(21), 5152.
[20] Torrez-Herrera, J. J., Fuentes-Ordoñez, E. G., Korili, S. A., & Gil, A. (2021). Evidence for the synthesis of La-hexaaluminate from aluminum-containing saline slag wastes: Correction of structural defects and phase purification at low temperature. *Powder Technology*, *377*, 80-88.
[21] Liu, W., Pouvreau, M., Stack, A. G., Yang, X., & Clark, A. E. (2022). Concentration dependent interfacial chemistry of the NaOH (aq): gibbsite interface. *Physical Chemistry Chemical Physics*, *24*(35), 20998-21008.
[22] Graham, T. R., Gorniak, R., Dembowski, M., Zhang, X., Clark, S. B., Pearce, C. I., ... & Rosso, K. M. (2020). Solid-state recrystallization pathways of sodium aluminate hydroxy hydrates. *Inorganic Chemistry*, *59*(10), 6857-6865.
[23] Hausmann, J. N., Traynor, B., Myers, R. J., Driess, M., & Menezes, P. W. (2021). The pH of aqueous NaOH/KOH solutions: a critical and non-trivial parameter for electrocatalysis. *ACS Energy Letters*, *6*(10), 3567-3571.
[24] Nienhuis, E. T., Pouvreau, M., Graham, T. R., Prange, M. P., Page, K., Loring, J. S., ... & Wang, H. W. (2022). Structure and reactivity of sodium aluminate complexes in alkaline solutions. *Journal of Molecular Liquids*, *367*, 120379.
[25] Takei, S., Kinoshita, H., & Murase, T. (2025). Application of Energy-Dispersive X-Ray Fluorescence Spectrometry for Examination of Foreign Bodies in Forensic Practice.
[26] A. S. Deepi, S. D. Priya, C. E. F. Christy, and A. S. Nesaraj. (2022). Facile Synthesis, Analysis of Physico-Chemical Properties and Tape Casting of Al2O3 Nanoparticles, *Asian J. Chem.*, vol. 34, no. 10, pp. 2651–2656.

[27] Marinos, D., Kotsanis, D., Alexandri, A., Balomenos, E., & Panias, D. (2021). Carbonation of sodium aluminate/sodium carbonate solutions for precipitation of alumina hydrates—avoiding dawsonite formation. *Crystals*, *11*(7), 836.

[28] Fadhilah, N., Muharja, M., Risanti, D. D., Wahyuono, R. A., Satrio, D., Khamil, A. I., & Fadilah, S. N. (2023). Kinetic study of the aluminum–water reaction using NaOH/NaAlO2 catalyst for hydrogen production from aluminum cans waste. *Bulletin of Chemical Reaction Engineering & Catalysis*, *18*(4), 615-626.

[29] Pedroza-Solis, C. D., De la Rosa, J. R., Lucio-Ortiz, C. J., Del Río, D. A. D. H., González-Casamachin, D. A., García, T. C. H., ... & Rangel, L. S. (2021). Thermocatalytic degradation of lignin monomer coniferyl aldehyde by aluminum–boron oxide catalysts. *Comptes Rendus. Chimie*, *24*(S1), 1-17.

[30] Mashkovtsev, M., Tarasova, N., Baksheev, E., Rychkov, V., Zhuravlev, N., Solodovnikova, P., & Galiaskarova, M. (2023). Spectroscopic study of five-coordinated thermal treated alumina formation: FTIR and NMR applying. *International Journal of Molecular Sciences*, *24*(6), 5151.

[31] Dembowski, M., Prange, M. P., Pouvreau, M., Graham, T. R., Bowden, M. E., Schenter, G. K., ... & Pearce, C. I. (2020). Inference of principal species in caustic aluminate solutions through solid-state spectroscopic characterization. *Dalton Transactions*, *49*(18), 5869-5880.

[32] Kabekkodu, S. N., Dosen, A., & Blanton, T. N. (2024). 5+: a comprehensive powder diffraction file™ for materials characterization. *Powder Diffraction*, *39*(2), 47-59.

[33] Proskurnina, N. V., Voronin, V. I., Shekhtman, G. S., & Kabanova, N. A. (2020). Crystal structure of NaFeO2 and NaAlO2 and their correlation with ionic conductivity. *Ionics*, *26*(6), 2917-2926.

[34] Durai, L., Gopalakrishnan, A., & Badhulika, S. (2022). Solid-state synthesis of β-NaAlO 2 nanoflakes as an anode material for high-performance sodium-ion batteries. *Materials Chemistry Frontiers*, *6*(19), 2913-2920.